Transparent materials for planar microelectrode arrays

Bc. Jaromír Jarušek
Department of Microelectronics
Brno University of Technology
Brno, Czech Republic
Jaromir.Jarusek@vutbr.cz

Ing. Jan Brodský
Department of Microelectronics
Brno University of Technology
Brno, Czech Republic
Jan.Brodsky@vutbr.cz

Ing. Imrich Gablech, Ph.D.
Department of Microelectronics
Brno University of Technology
Brno, Czech Republic
Imrich.Gablech@vutbr.cz

***Abstract*—This paper is focused on indium tin oxide (ITO), ultrathin gold, titanium nitride (TiN) and diamond-like carbon (DLC) thin films that can be used for transparent or semitransparent electrodes and interconnects for planar microelectrode arrays. Paper further describes methods of thin film deposition of selected materials, microfabrication of planar microelectrode arrays, their preparation for electrochemical measurement and results of electrochemical impedance spectroscopy and cyclic voltammetry.**

Keywords— planar microelectrode array (pMEA) indium tin oxide (ITO), titanium nitride, diamond like carbon (DLC), ultrathin gold thin film, electrochemical impedance spectroscopy

I. Introduction

Planar microelectrode arrays (pMEAs) are devices for *in vitro* research of electrogenic cells, i.e. electrically active cells. Those include neurons, heart cells (cardiomyocytes), retinal cells and smooth muscle cells. They are important tools for neural electrophysiology and investigations of neural network signaling and neural plasticity, more general applications include toxicity testing and drug screening. [1], [2], [3] *In vitro* drug screening is especially important for pharmacological applications because some drugs for disease treatment, unrelated to cardiac diseases, can cause life-threatening cardiac rhythm disturbances (arrhythmias). The usage of pMEAs for this application presents an easier and efficient method in comparison to approaches such as isolated Purkinje fibers or *ex vivo* Langendorff heart. [4]

For cell studies inverted optical microscope is preferred, since observation from top may not be possible, because of presence of culturing medium. The usage of opaque electrodes and interconnections limits the view, thus usage of transparent or semitransparent electrodes is desirable for such applications. [5].

In the field of commercial pMEAs it is common that electrode materials and even materials of interconnects are opaque. [2] Some of the examples are MCS 60MEA with opaque TiN and advertised impedance of < 100 kΩ for 30 µm electrode diameter or MED64 with platinum black electrodes with advertised impedance of 10 kΩ for 30 µm electrode diameter. [6], [7]

The only commercial pMEA, with advertised transparent electrodes, is MCS 120tMEA with advertised impedance of < 250 kΩ and utilization of semitransparent TiN. Specified diameter of electrodes is 100 µm. [8] Further information about used TiN layer, such as thickness or optical transmittance, is not known. It could also be pointed out that if electrode diameter 100 µm is not an error in documentation, guaranteed impedance of < 250 kΩ is relatively high.

II. Materials for microfabrication of pMEAs

Two approaches were employed to fabricate semitransparent electrodes and interconnects. The former utilizes ultrathin ≈ 9 nm gold layer as a main conductor, and latter uses highly transparent ITO layer with low sheet resistance as a main conductor and different material which may have significantly higher sheet resistance, but has better chemical, electrochemical, or other properties. As a source of ITO, commercially available 4" ITO coated glass wafers with advertised sheet resistance < 10 $\Omega \cdot \square^{-1}$ were used. The value of sheet resistance has been verified to be in range from 6.5 $\Omega \cdot \square^{-1}$ to 7.8 $\Omega \cdot \square^{-1}$ for different wafers. Besides ITO other materials were deposited in vacuum systems in CEITEC Nano cleanrooms.

A. Deposition of thin semitransparent conductive films

Prior to depositions, all substrates were cleaned in ultrasonic bath using acetone and isopropyl alcohol with subsequent rinse with deionized water. Further cleaning was performed using oxygen plasma in Diener plasma cleaner and finally *in situ* Ar ions precleaning was utilized just prior to deposition in respective deposition systems.

For deposition of semitransparent gold layer, a borofloat wafer was used. To enhance adhesion to the substrate, ≈ 1 nm of titanium was sputtered before gold in the same process and the same deposition parameters, without breaking the vacuum. The semitransparent gold layer with thickness of ≈ 9 nm was deposited using ion-beam sputtering technique. The thickness of ≈ 9 nm was chosen as a compromise between sheet resistance, which steeply rises below 10 nm, and optical transmittance, which is around 50 % at 10 nm. [9] The deposition was performed in system equipped with two Kaufman & Robinson RFICP40 ion-beam sources. Energy of ion beam was 600 eV and current 44 mA.

Similarly to the semitransparent gold layer, 1 nm of titanium was sputtered as adhesion layer under TiN. TiN layer with thickness of ≈ 20 nm was deposited using ion-beam assisted deposition using both ion-beam sources. This process was described in more detail in previous publications. Deposition was carried out in temperatures < 100 °C with process

parameters as follows. Energy of primary beam was 600 eV, primary beam current was 44 mA, primary beam gas supply was a mixture of argon and nitrogen with mass flows 3.6 sccm and 3 sccm respectively. Energy of secondary beam was 26 eV and secondary beam current was 15 mA.[10], [11]

DLC layer with thickness of ≈ 150 nm was deposited directly on precleaned ITO layer by plasma-enhanced chemical vapor deposition (PECVD) using Oxford Instruments PlasmaPro 80 RIE system. Layer was deposited from CH_4 plasma. Deposition was carried out at an elevated temperature of ≈ 60 °C and working pressure of ≈ 53.3 Pa at the corresponding deposition rate of ≈ 8 nm·min^{-1}. [12]

B. Optical transmittance of used films

Optical transmittance was measured using three-channel optical spectroscope Ocean Insight JAZ3 and extracted results are shown in Fig. 1. It is apparent that ITO has the highest optical transmittance in the visible range out of all investigated conductive layers. An interesting result is the DLC layer on ITO, because decrease in transmittance compared to ITO layer alone is only small. DLC on ITO layers could with combination of good electrical and electrochemical properties present very interesting material combination for transparent pMEA. This is in contrast to TiN with average transmittance ≈ 45 % and ultrathin gold thin film with average transmittance ≈ 55 %, that can serve only as semitransparent conductors. For further comparison DLC-ITO layer has transmittance on par with other optical parts of pMEA like encapsulation consisted of 50 nm AlN and 3 µm of Parylen-C.

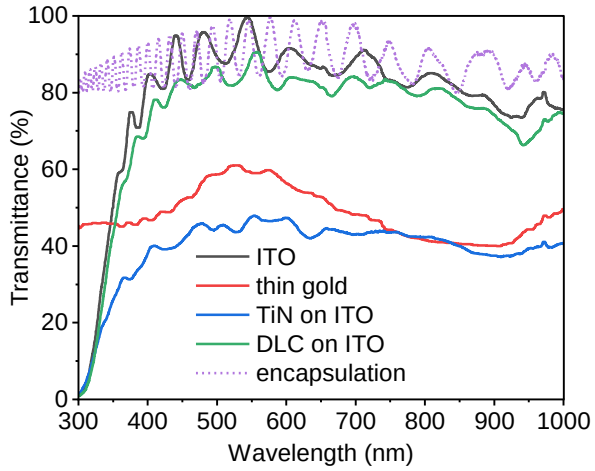

Fig. 1. Graph of optical transmittances of prepared thin films.

III. Microfabrication of pMEAs

A. Description of used design

Design consisting of three photolithographic masks was used for microfabrication of pMEAs. Illustration of pMEA design is shown in Fig. 2. First mask contains a pattern for transparent electrodes and underlying interconnects. The second mask contains a pattern for gold metallization of pads and interconnects outside of the active diameter which is comparable with field of view of 10x microscope objectives. Pattern of the third mask allows the creation of opening in deposited encapsulation for pads and transparent electrodes.

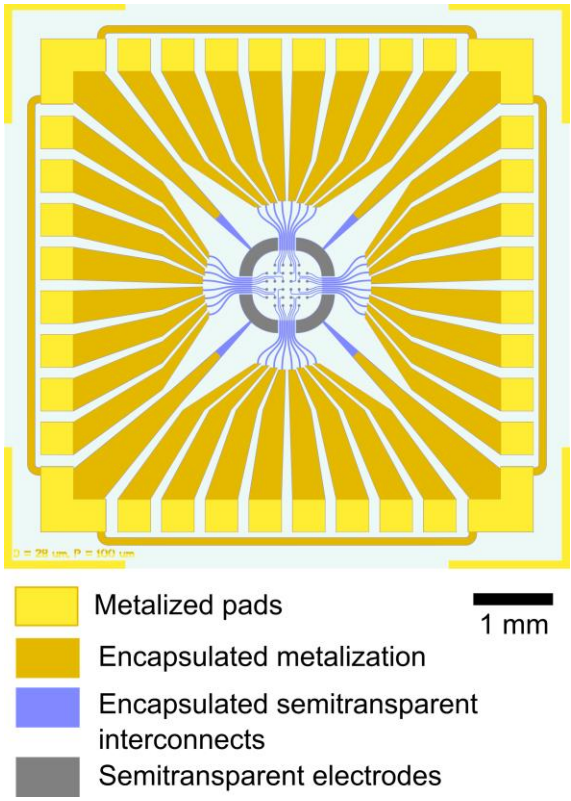

Fig. 2. Design of pMEA chip with pitch of 100 µm. Parts conductive pattern are highlighted with colors.

Used masks contain four variants of pMEA design, where pitches between microelectrodes are 100 µm and 200 µm and diameters of microelectrodes are 30 µm and 50 µm. The variant with 100 µm pitch and 30 µm is illustrated in Fig. 2.

B. Photolithographic process

pMEAs were fabricated at CEITEC Nano class 100 cleanrooms. Photolithography was performed using semiautomated coating system SÜSS MicroTec RCD8 and a mask aligner SÜSS MicroTec MA8 Gen3. All etching processes were performed using plasma processes, specifically by ion beam etching using Scia Systems Coat 200 and reactive ion etching using Oxford Instruments Plasma Technology PlasmaPro 100 and PlasmaPro 80. For etching using ion beam, AZ MIR 701 type photoresist spincoated at 4000 rpm was used. Ion beam etching was used for gold and DLC layers.

Workflow of fabrication of conductive pattern had varied for different materials. In case of ultrathin film gold electrodes, semitransparent thin film was deposited after pad and interconnection metallization. In case of TiN, underlying ITO pattern was etched first and subsequently TiN thin film was deposited. DLC on ITO was etched using same lithography using ion beam etching and subsequently reactive ion etching.

After completion of conductive pattern, encapsulation layers were deposited. First, a 50 nm aluminum nitride (AlN) thin film was sputtered using two ion beam assisted deposition, then 3 µm of Parylene-C was deposited using SCS Parylene Deposition System. For etching of opening in encapsulation for pads and

microelectrodes, thick photoresist AZ 1518 spincoated at 1000 rpm was used. Parylene-C was etched using oxygen plasma and AlN was etched using mixture of BCl_3 and Cl_2 plasma.

Before the wafers dicing a photoresist was spincoated on the wafer for protection during dicing process. An example of the results of manufactured pMEA is in Fig. 3.

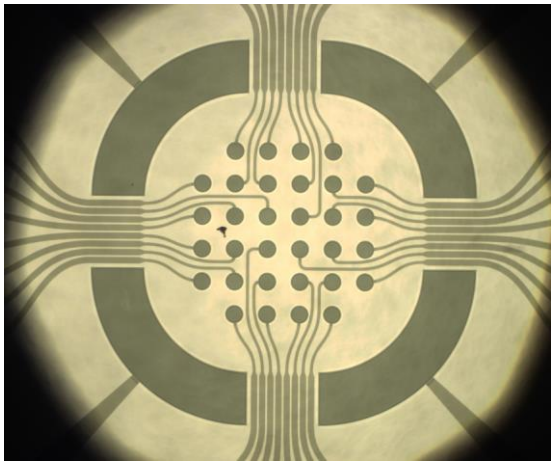

Fig. 3. Example of manufactured pMEA under optical microscope in transmitted light.

IV. Electrochemical Characterization

A. pMEAs preparation

In order to use the fabricated chips for measurements, several preparatory steps were required. First, the chips were cleaned using the following cleaning procedure. The chip held by the tweezers was rinsed with acetone using a washing bottle to wash away the debris from dicing. Then, the chip was moved to a beaker with acetone, where it was agitated in an inclined position for better removal of the protective photoresist. To completely clean the residual impurities, the chip was left in pure acetone for 5 minutes, another 5 minutes in isopropyl alcohol, followed by rinse with pure isopropyl alcohol by agitating in a beaker, and dried with compressed air. Proper results of cleaning procedure were verified using a microscope.

Second step involves fixing of the chip in the open cavity of ceramic leadless chip carrier (LCC) package using a small amount of molten wax. The pads of pMEAs were then electrically connected to the package using wirebonding method. Wirebonding was done using TPT HB16 wire bonder in wedge bonding setup with gold wire.

The last step involves attaching a small well to the chip for holding electrolyte or cell culture medium. Wells were made using fused filament fabrication (FFF) 3D printing from polyethylene terephthalate glycol (PETG) filament. Wells have internal dimensions $\approx (3.3\times3.3)\ mm^2$, wall thickness of $\approx$ 0.45 mm, and height $\approx$ 6 mm. Attachment was done manually by applying tiny amount of polydimethylsiloxane (PDMS) on base edge of well and then placing it on pMEA using tweezers. Applied PDMS was partially cured in oven at temperatures around 80 °C. Another dose of PDMS was applied to enhance watertightness and attachment robustness. PDMS was applied on the rest of chip outside the well, including pads and wire bonds, and then cured in oven at temperatures around 80 °C for 30 minutes. Illustration of pMEA prepared for electrochemical measurements is in Fig. 4.

A different approach was used for ITO-only microelectrodes chips, where issues with wirebonding reliability were encountered. This limited amount of measurement results.

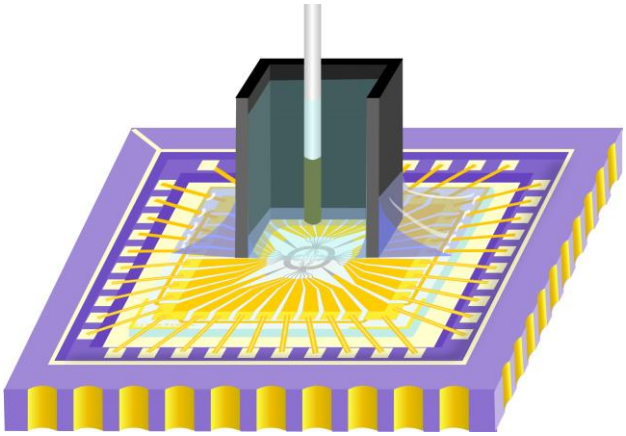

Fig. 4. Cross-section of pMEA prepared for electrochemical measurements.

B. Electrochemical measurements

Prepared pMEAs, as depicted in Fig. 4, were placed into platform with connectors and socket for the LCC package. As an electrolyte for electrochemical measurement, a 0.1M KCl solution was used. The solution was applied using micropipette. In case of ITO chip, pMEA was rinsed with ethanol before application of the 0.1M KCl solution. A silver wire with electrodeposited AgCl tip was used as a pseudoreference electrode.

Electrochemical measurements were performed using Metrohm Autolab III potentiostat. Measurements consisted of 5 cycles of electrochemical impedance spectroscopy interlaced with 10 cycles of cylic voltammetry in range (−0.3 +0.5) V relative to the Ag/AgCl pseudoreference electrode. For the measurements, pMEAs with 50 µm microelectrode diameter and, in most cases, with 100 µm pitch were selected.

V. Results of Electrochemical Measurements

From Fig. 5, it can be concluded that 9 nm gold, 20 nm TiN on ITO and 150 nm DLC on ITO exhibit similar impedance magnitudes down to 10 Hz, whereas the ultrathin gold layer deviates to higher magnitudes at lower frequencies. Bare ITO electrodes exhibit significantly higher impedance across the entire frequency spectrum. From Fig. 6, it can be further observed that double layer capacitance is so low that series resistance of electrochemical system is not clearly apparent even at high frequencies.

These characteristics can also be seen in cyclic voltammograms in Fig. 7. Both TiN and DLC have similar capacitive curves with a larger area under the curves, that suggests higher double layer capacitance than gold and bare ITO. Impedances for ultrathin gold, semitransparent TiN and DLC were found to be $\approx$ 700 kΩ.

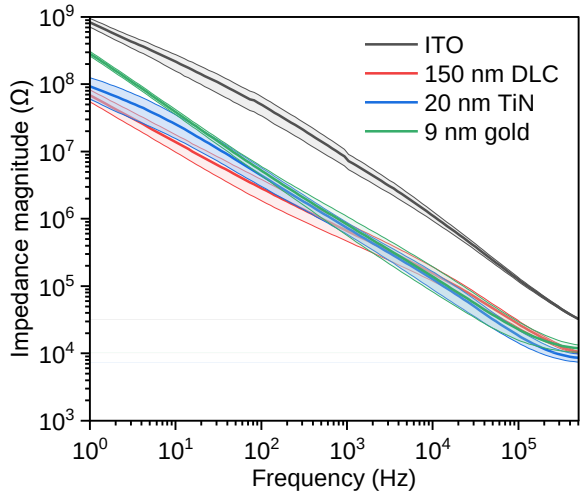

Fig. 5. Statistical results of electrochemical impedance spectroscopy – impedance magnitude.

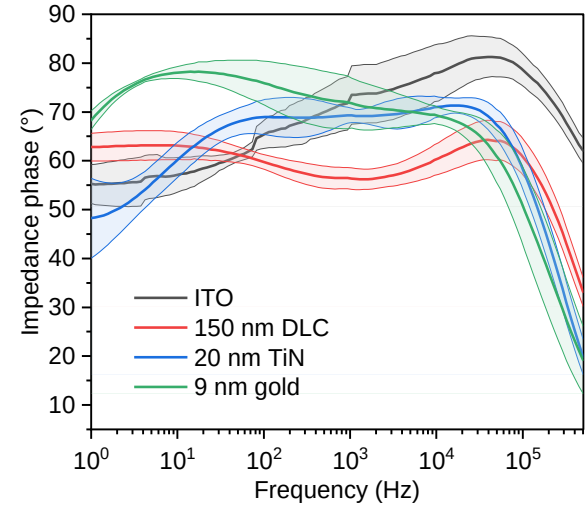

Fig. 6. Statistical results of electrochemical impedance spectroscopy – impedance phase.

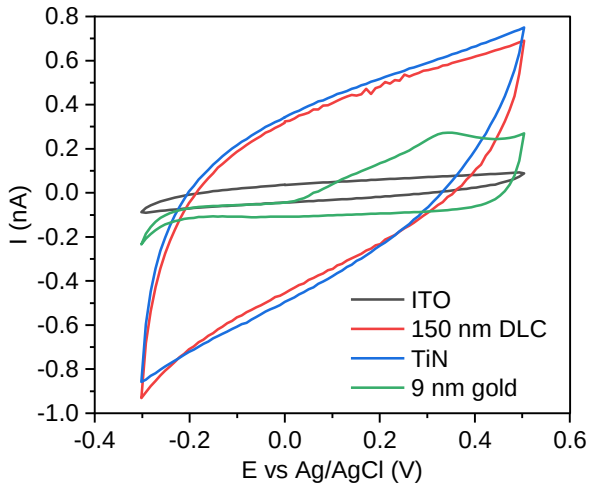

Fig. 7. Averaged steady-state cyclic voltammograms.

VI. Conclusion

From measured optical transmittances and electrochemical measurements, it can be concluded that DLC on ITO layer has very interesting properties in comparison to other investigated materials. Further investigation of DLC layers is important to better evaluate the potential for practical use as material with superior properties for pMEAS. Further optimization of TiN and DLC layers is desirable for more competitive performance.

Acknowledgment

CzechNanoLab project LM2023051 funded by MEYS CR is gratefully acknowledged for the financial support of the measurements/sample fabrication at CEITEC Nano Research Infrastructure.

References

[1] H. S. Jeong, S. Hwang, K. S. Min, and S. B. Jun, "Fabrication of Planar Microelectrode Array Using Laser-Patterned ITO and SU-8", *Micromachines*, vol. 12, no. 11, 2021.

[2] M. -G. Liu, X. -F. Chen, T. He, Z. Li, and J. Chen, "Use of multi-electrode array recordings in studies of network synaptic plasticity in both time and space", *Neuroscience Bulletin*, vol. 28, no. 4, pp. 409-422, 2012.

[3] A. Koklu, R. Atmaramani, A. Hammack, A. Beskok, J. J. Pancrazio, B. E. Gnade, and B. J. Black, "Gold nanostructure microelectrode arrays for in vitro recording and stimulation from neuronal networks", *Nanotechnology*, vol. 30, no. 23, Jun. 2019.

[4] A. Stett, U. Egert, E. Guenther, F. Hofmann, T. Meyer, W. Nisch, and H. Haemmerle, "Biological application of microelectrode arrays in drug discovery and basic research", *Analytical and Bioanalytical Chemistry*, vol. 377, no. 3, pp. 486-495, Oct. 2003.

[5] T. Ryynänen, R. Mzezewa, E. Meriläinen, T. Hyvärinen, J. Lekkala, S. Narkilahti, and P. Kallio, "Transparent Microelectrode Arrays Fabricated by Ion Beam Assisted Deposition for Neuronal Cell In Vitro Recordings", *Micromachines*, vol. 11, no. 5, 2020.

[6] "MED Probe (MEA)" https://www.med64.com/products/med-probe-mea/ (accessed Apr. 01, 2024)

[7] "60StandardMEA", multichannelsystems.com. https://www.multichannelsystems.com/sites/multichannelsystems.com/files/MCS_60StandardMEA_Layout.pdf (accessed Apr. 1AD)

[8] "120tMEA100/30iR-ITO," 2019. https://www.multichannelsystems.com/sites/multichannelsystems.com/files/documents/data_sheets/120tMEA100-30-ITO_Layout.pdf (accessed Apr. 01, 2024)

[9] S. Wilken, T. Hoffmann, E. von Hauff, H. Borchert, and J. Parisi, "ITO-free inverted polymer/fullerene solar cells: Interface effects and comparison of different semi-transparent front contacts", *Solar Energy Materials and Solar Cells*, vol. 96, pp. 141-147, 2012.

[10] J. Jarušek, "Naprašování nitridových vrstev pro bioelektronické aplikace pomocí Kaufmanova iontového zdroje", Bakalářská práce, Brno, 2022.

[11] I. Gablech, L. Migliaccio, J. Brodský, M. Havlíček, P. Podešva, R. Hrdý, J. Ehlich, M. Gryszel, and E. D. Głowacki, "High-Conductivity Stoichiometric Titanium Nitride for Bioelectronics", *Advanced Electronic Materials*, vol. 9, no. 4, 2023.

[12] O. Sharifahmadian, A. Pakseresht, S. Mirzaei, M. Eliáš, and D. Galusek, "Mechanically robust hydrophobic fluorine-doped diamond-like carbon film on glass substrate", *Diamond and Related Materials*, vol. 138, 2023.